12

Heat Transfer in the Transitional Flow Regime

JP Meyer and JA Olivier
University of Pretoria,
Department of Mechanical and Aeronautical Engineering,
South Africa

1. Introduction

Transitional flow, whereby the motion of a fluid changes from laminar to turbulent flow, was successfully identified by Reynolds (1883) almost 130 years ago. According to ASHRAE (2009), for a round pipe, in general, laminar flow exists when the Reynolds number is less than 2 300. Fully turbulent flow exists when the Reynolds number is larger than 10 000 and transitional flow exists for Reynolds numbers between 2 300 and 10 000. Despite much work on transition and even though it is of considerable importance in determining pressure drop and heat transfer in convective flow, the underlying physics and the implications of this phenomenon have eluded complete understanding (Obot et al., 1990).

ASHRAE further states that predictions are unreliable in the transitional flow regime. Cengel (2006) mentions that although transitional flow exists for Reynolds numbers between 2 300 and 10 000, it should be kept in mind that in many cases the flow becomes fully turbulent when the Reynolds number is larger than 4 000. It is normally advised when designing heat exchangers to remain outside the transitional flow regime due to the uncertainty and flow instability in this region. For this reason, little design information is available with specific reference to heat transfer and pressure drop data in the transitional flow regime.

It has been known that there is a relationship between pressure drop and heat transfer generally referred to as the Reynolds analogy. Therefore, the relationship between friction factor and Nusselt number was studied by many and an overview of all the contributions on the subject is given by Colburn (1933). Obot et al. (1990) followed up on this previous work to investigate the role of transition in determining friction and heat transfer in smooth and rough passages. Later on they (Obot et al., 1997) took measurements of heat transfer and pressure drop in smooth tubes in laminar, transitional and turbulent flow over a wide range of Prandtl numbers.

García et al. (2005) experimentally investigated helical wire coils fitted inside a round tube in order to characterise their thermohydraulic behaviour in laminar, transitional and turbulent flow. They did experiments over a wide range of Reynolds and Prandtl numbers and they found that at low Reynolds numbers, wire coils behave as a smooth tube but accelerate transition to critical Reynolds numbers down to 700. Furthermore, within the transition region, if wire coils are fitted inside a smooth tube heat exchanger, the heat transfer rate can be increased up to 200% while maintaining a constant pumping power. This is in comparison with the turbulent flow regime where wire coils increase pressure drop up to nine times and heat transfer up to four times compared with empty smooth

tubes. In a follow-up study, García et al. (2007) reported that at a Reynolds number of around 1 000, wire inserts increase the heat transfer coefficient up to eight times; while the friction factor increases with approximately 40%.

Furthermore, not only tube roughness and enhancement devices such as wire coils but also the geometry of the inlet of smooth tubes were found to have a significant influence on the transition Reynolds number. Ghajar and co-workers conducted extensive studies into the effect of three different types of inlets on the critical Reynolds number. Three of more than seven articles are those of Ghajar and Tam (1990; 1994; 1995). More recent work on the effect of different inlet geometries has been conducted by Mohammed (2009). However, his work was limited to the laminar flow regime for a Reynolds number range of 400 to 1 600. Furthermore, Ghajar and Tam's, as well as Mohammed's work, used a constant heat flux boundary condition, which heats and does not cool fluids in a tube and does not ensure a constant wall temperature as would occur with water flowing in the inside of the tubes of a shell-and-tube heat exchanger (as in the case of the current work). More differences between constant wall temperature and constant heat flux results and why the results are not comparable with this study are summarised in Olivier (2009).

The purpose of this chapter is to present a review of measured heat transfer and pressure drop data in the transitional flow regime of water flowing in a horizontal circular smooth tube and an enhanced tube while the temperature of the wall remains fairly constant. The constant wall temperature is the same operating condition experienced in water chillers where water is cooled in the inner tubes of a shell-and-tube heat exchanger with refrigerant boiling on the outside of water tubes.

2. Experimental set-up

A tube-in-tube heat exchanger in a counterflow configuration was used as the test section. Water was used as the working fluid for both streams (Fig. 1), with the inner fluid being hot and the annulus fluid being cold. The inlet tube temperature of the inner tube was 40-45°C and the annulus inlet temperature was 20 °C. Heating of the test fluid for the inner tube was done by means of a secondary flow loop containing water from a large reservoir. The temperature in this reservoir was maintained at approximately 60°C by means of an electric heater, while the reservoir for the annulus water was cooled with a chiller.

The test fluid was pumped through the system with two electronically controlled positive displacement pumps. The two pumps were installed in parallel and were used in accordance with the flow rate requirements. The cold water loop was connected to a second large reservoir, which again was connected to a chiller. The water was circulated through the system via an electronically controlled positive displacement pump. Coriolis flow meters were used to measure the mass flow rates.

Prior to the flow entering the test section, for three of the four different types of test sections, the flow first went through a calming section as shown schematically in Fig. 2. The purpose of the calming section was two-fold; first, to remove any unsteadiness in the flow and to ensure a uniform velocity distribution and, second, to house three of the four different types of inlets to be investigated. The calming section geometry was based on work conducted by Ghajar and Tam (1990) and consisted of a 5° diffuser, which increased from a diameter of 15 mm to 140 mm. This angle was chosen such to prevent flow separation from the diffuser wall. Three screens were placed after the diffuser with an open-area ratio (OAR) of 0.31. The OAR is the ratio of the area occupied by the holes to the total area occupied by the whole screen. A honeycomb section, which had an OAR of 0.92, followed the screens.

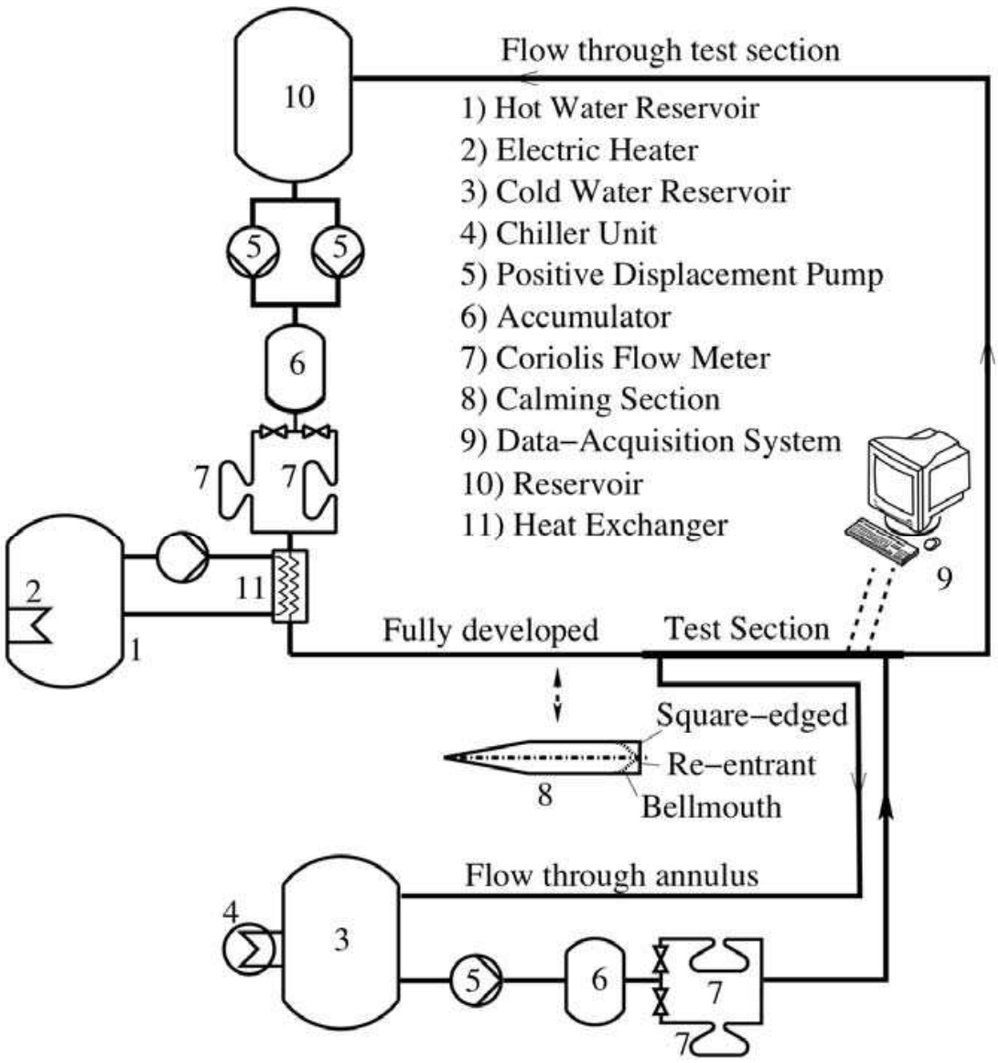

Fig. 1. Schematic layout of the experimental system

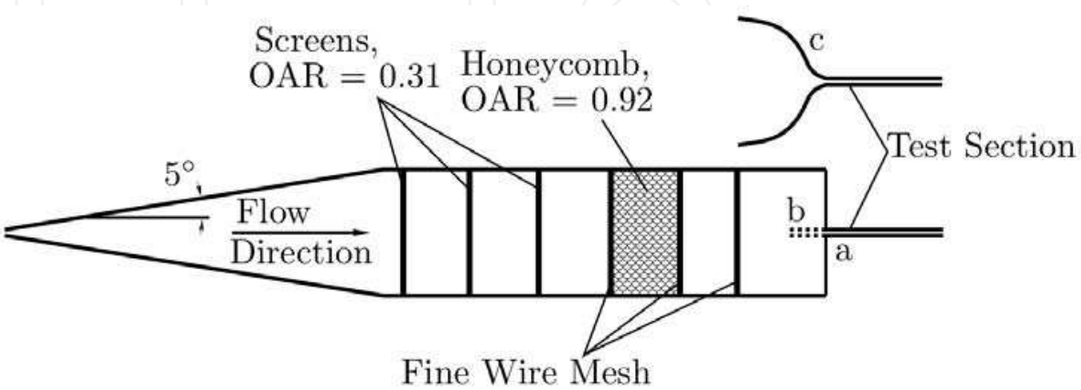

Fig. 2. Calming section with the different types of inlet configurations: a) square-edged, b) re-entrant and c) bellmouth

Prior to and after the honeycomb, a wire mesh was placed with the wires having a diameter of 0.8 mm and the OAR being 0.54. Another fine wire mesh was inserted between the last honeycomb mesh and the test inlet. This mesh had a wire diameter of 0.3 mm and an OAR of 0.17.

Three different inlets (Fig. 3) could be housed on the calming section, namely a square-edged, re-entrant and bellmouth inlet. These inlets are also shown in Fig. 2 as items a, b and c, respectively. The calming section was designed such that the inlets could easily be interchanged. The square-edged inlet is characterised by a sudden contraction of the flow. This is a typical situation encountered in the header of a shell-and-tube exchanger.

The re-entrant inlet makes use of the square-edged inlet except that the tube slides into the inlet by one tube diameter. This would simulate a floating header in a shell-and-tube heat exchanger.

The third type of inlet is the bellmouth. The bellmouth is characterised by a smooth contraction, having a contraction ratio of 8.8. The shape of the bellmouth was calculated with the method suggested by Morel (1975). The use of a bellmouth is thought to help in the reduction of fouling, although practical application thereof is uncommon in heat exchangers.

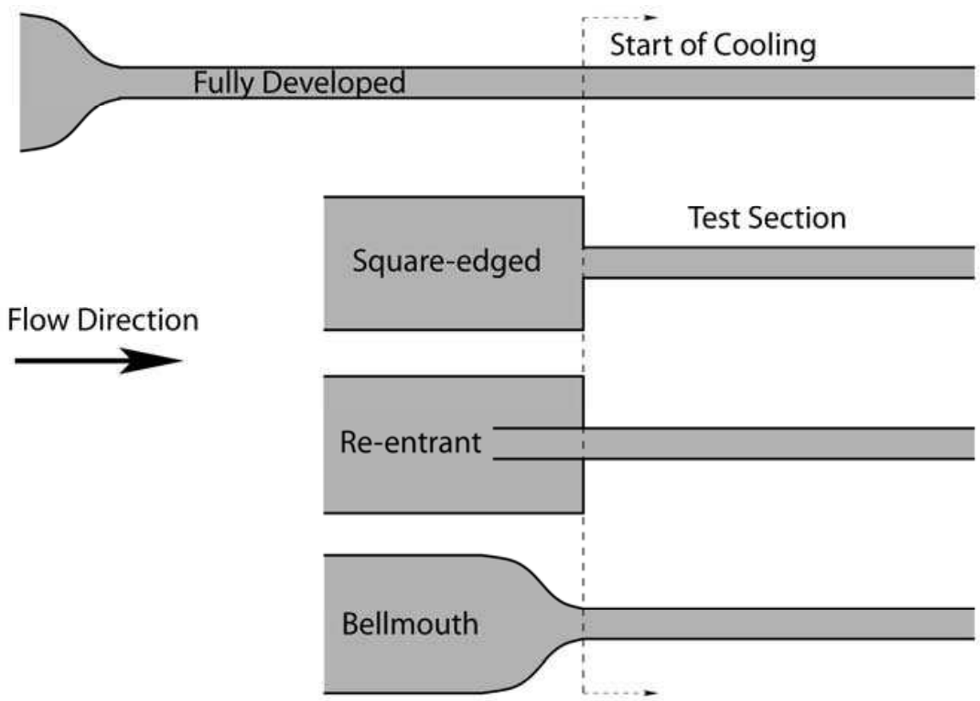

Fig. 3. Illustration of the different inlet geometries relative to the test section

The fourth type of inlet used was a fully developed inlet, which did not make use of the calming section. This inlet had an inner diameter being the same as that of the test section. The length of the fully developed inlet was determined in terms of the suggestion by Durst et al. (2005), which required a minimum length of 120-tube diameters. To ensure this minimum was met, the length of the inlet was chosen as 160-tube diameters. Cooling started, in the case of adiabatic tests, after this inlet section, while for the other inlets, cooling started after the calming section.

All the insulated test sections (Fig. 4) were operated in a counterflow configuration and were manufactured from hard-drawn copper tubes. The total length of each test section was approximately 5 m. The tubes tested had a nominal outside diameter of 15.88 mm and inner diameter of 14.482 mm. The outer-wall diameters of the enhanced tubes were 15.806 mm and the inner-wall diameters were 14.648 mm. It had fins with a height of 0.395 mm with a fin apex angle of 43.93°. The one tube had 25 fins with a helix angle of 18°, while the other had 35 fins with a helix angle of 27°. More details of the fins are available in Olivier (2009) and Meyer and Olivier (2011a).

The annulus mass flow was high, which ensured that the wall temperature of the inner tube remained relatively constant for most experiments. The annulus inner diameter of 20.7 mm was chosen such that the space between the annulus and the inner tube was small, ensuring high flow velocities and thus turbulent flow in the annulus, which further ensured that the annulus had a small thermal resistance compared with that of the inner tube. To prevent sagging and the outer tube touching the inner tube, a capillary tube was wound around the outer surface of the inner tube at a constant pitch of approximately 60°. This also further promoted a rotational flow velocity inside the annulus, producing a higher heat transfer coefficient and thus low thermal resistance.

A full experimental uncertainty analysis (Table 1) was performed on the system using the method suggested by Kline and McClintock (1953). Uncertainties for the calculated Nusselt numbers were less than 2% and for the friction factor they were less than 12% for low Reynolds numbers (less than 1 000) but less than 3% at a Reynolds number of approximately 15 000.

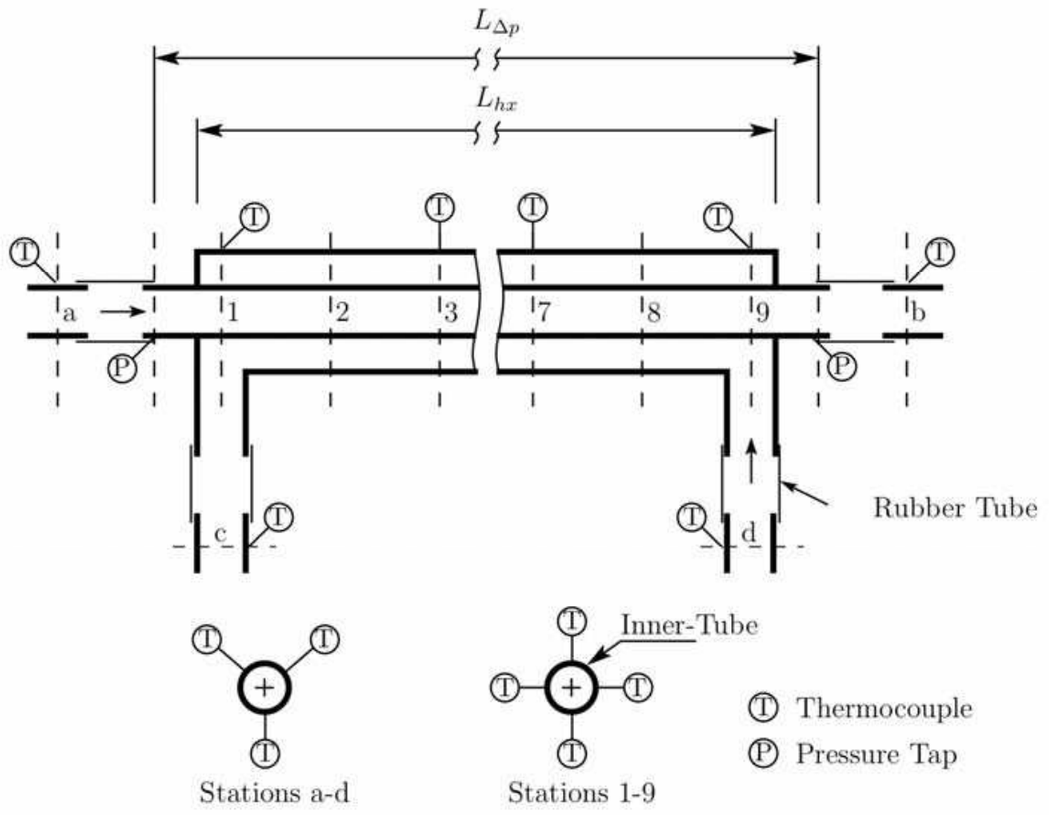

Fig. 4. Schematic layout of the test section

3. Data reduction

The inner tube's average heat transfer coefficient was obtained by making use of the overall heat transfer coefficient and the sum of the resistances, given by

$$\alpha_i = \frac{1}{A_i}\left[\frac{1}{UA} - R_w - \frac{1}{\alpha_o A_o}\right]^{-1} \tag{1}$$

UA is the overall heat transfer coefficient, which can be obtained by means of the overall heat transferred and the log-mean temperature difference, calculated from the inlet and outlet temperatures of the inner tube and annulus

$$UA = \frac{\dot{Q}_i}{T_{lmtd}} \tag{2}$$

$\dot{Q}_i$ is the heat transferred in the inner tube, calculated as

$$\dot{Q}_i = \dot{m}_i C_p \Delta T \tag{3}$$

while $\dot{m}_i$ and ΔT are, respectively, the inner-tube mass flow rate and the temperature difference between the in- and outlet of the inner tube. The specific heat values were obtained from IAPWS (2003), which are based on the fluid temperature. The annulus heat transfer coefficient was calculated by means of the annulus bulk temperature and the average inner-tube outer-wall temperature measurements. The bulk and average wall temperatures were obtained by making use of the trapezium rule to "integrate" over the whole length of the tube. Therefore, only a single bulk value for the annulus heat transfer coefficient was obtained. This is given by

$$\alpha_o = \frac{\dot{Q}_i}{A_o\left(T_o - T_{wo}\right)} \tag{4}$$

The inner-tube heat transfer rate was used for all the calculations since it had the lowest uncertainty. Throughout the tests, the annulus flow rate was kept as high as possible as this reduced the thermal resistance of the annulus, reducing its influence in Eq. (1) and hence decreasing the equation's overall uncertainty. On average, the annulus thermal resistance was only 6% the value of the inner tube. All fluid properties were obtained from Wagner and Pruß (2002). Experimental data were only captured once an energy balance of less than 1% was achieved. At low inner-tube Reynolds numbers (<6 000), this requirement was not met due to the high annulus flow rate and its uncertainty. Tests were, however, conducted as checks by substantially lowering the annulus flow rate. These tests proved that the heat transfer error in the inner tube at low Reynolds numbers was indeed less than 1%.
The Darcy-Weisbach friction factors were determined by

$$f = \frac{2\Delta p D_i}{\rho u^2 L_{\Delta p}} \tag{5}$$

The bulk fluid properties used for the calculation of the Reynolds, Prandtl numbers, etc., were calculated at the average inner-tube fluid temperature, which, in turn, was determined by the resulting heat transfer coefficient, Eq. (1), as

$$T_i = \frac{\dot{Q}_i}{\alpha_i} + T_{wi} \tag{6}$$

Property	Value	Uncertainty
$\dot{m}_i$	0.0087 - 0.0822	0.664 - 0.412%
$\dot{m}_o$	0.429 - 0.445	0.164 - 0.260%
T_{iin}, T_{iout}, T_{oin}, T_{oout}	20.35 - 65.67	0.011 - 0.46
T_o	20.9 - 23.67	0.014 - 0.032
T_{wo}	21.33 - 25.53	0.011 - 0.055
T_{wi}	21.34 - 25.61	0.011 - 0.055
T_i	32.98 - 41.97	0.176 - 0.857
T_{lmtd}	12.16 - 18.18	0.172 - 0.855
$\dot{Q}_i$	1 598 - 10 954	0.71 - 0.49%
UA	131.5 - 605.8	1.02 - 1.08%
Re	1 026 - 11 485	1.20 - 1.08%
Nu	13.06 - 62.20	1.44 - 1.58%
Pr	4.17 - 5.06	±1.42%
Δp	45 - 1 583	4.71 - 1.59%
α_i	558 - 2 710	1.04 - 1.22%
f	0.0085 - 0.0212	2.84 - 11.28%

Table 1. Experimental range and uncertainties

4. Results

In this section, the results are given. The experimental results are first validated for smooth tubes, by presenting friction factor data without heat transfer, whereafter the diabatic friction factors are given, followed by the heat transfer results in the form of Nusselt numbers. Lastly, the friction factors and heat transfer results of enhanced tubes are given.

4.1 Validation for smooth tube

Figure 5 shows the adiabatic friction factor results with various inlet profiles. This figure shows how the transition region is manipulated by the use of different types of inlets (Olivier and Meyer, 2010). The square-edged inlet delays transition to Reynolds numbers of around 2 600, while the bellmouth inlet delays it to about 7 000. Transition for the re-entrant inlet did not differ much from the fully developed inlet. Thus, the smoother the inlet, the more delayed is transition.

Laminar flow results for the various inlets, unlike the fully developed results, are slightly higher than the laminar friction factor obtained from the Poiseuille relation.

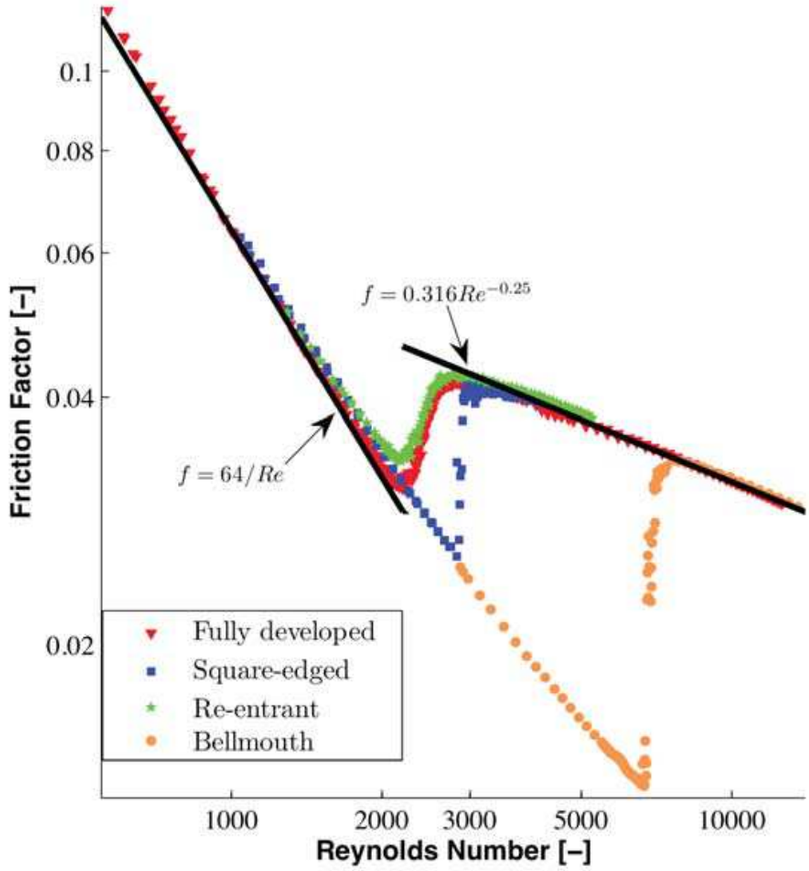

Fig. 5. Adiabatic friction factors for the smooth tube with various inlets

4.2 Diabatic friction factor for smooth tube

Since it has been shown that viscosity differences between the bulk of the fluid and the fluid at the wall have an effect on friction factors (Sieder and Tate, 1936), it is of importance to report on the diabatic friction factors as well. This is further substantiated by the fact that there is a secondary flow component present (Tam and Ghajar, 1997). The presence of this secondary flow is shown in Fig. 6 with regard to the laminar and transition regions for all the different inlets of the two diameter tubes. Plotted on the graph are the experimental friction factors for the smooth tube during fully developed flow, the laminar Poiseuille relation, the turbulent Blasius equation and the correlation of Filonenko (1948), which is also given by Lienhard and Lienhard (2003) and more commonly used in the heat transfer correlation of Gnielinski (1976).

Turbulent flow results correlated fairly well with the viscosity ratio correction, although it would seem as if full turbulence is only reached at Reynolds numbers above 15 000. Unfortunately, the range of data was limited such that this could not be confirmed by taking measurements at Reynolds numbers greater than 15 000. For the laminar flow region, friction factors were on average 35% higher than predicted by the Poiseuille relation. Even with a viscosity correction, the prediction only improved by 4%. This increase in friction factor can be attributed to the secondary flow effects, with data from Nunner (1956) showing similar results. Tam and Ghajar (1997) also noted this increase and found that it was dependent on the heating rate. This implies that since the friction factor is proportional

to the wall shear stress, which, in turn, is proportional to the velocity gradient at the wall, secondary flows distort the velocity profile in such a way that the velocity gradient near the wall is much greater. This would then give rise to the higher friction factors. Many numerical and experimental studies have been performed showing this distortion (Mikesell 1963; Faris and Viskanta 1969; Hishida *et al*., 1982).

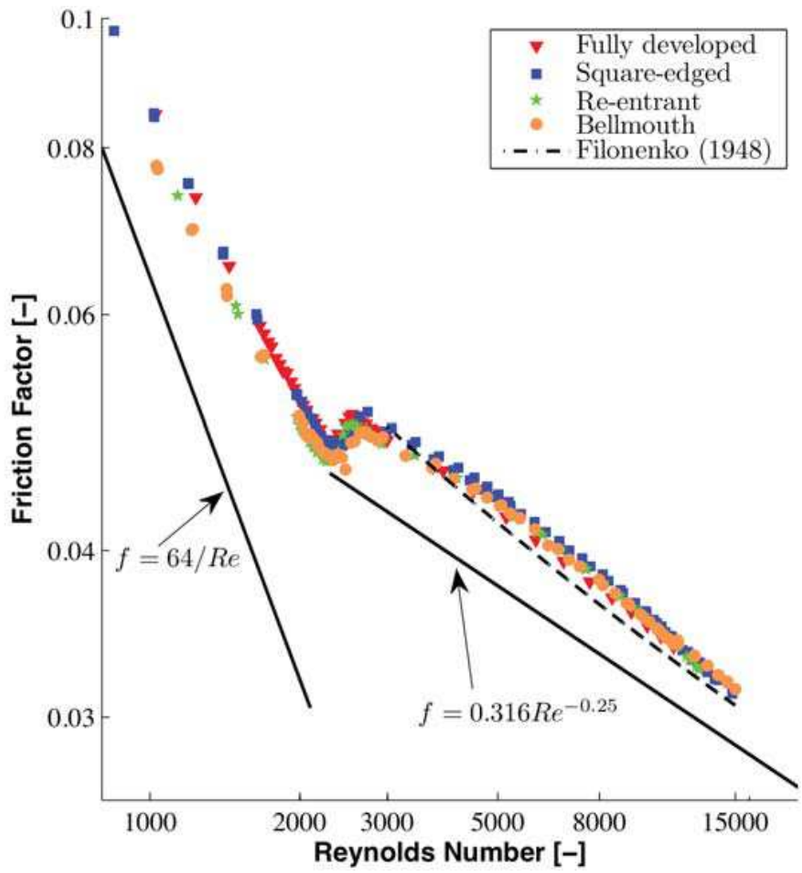

Fig. 6. Diabatic friction factors for the smooth tubes with various inlets

4.3 Nusselt numbers for smooth tube

Figure 7 consists of a total of 261 data points of heat transfer results with a fully developed hydrodynamic boundary layer since the thermal boundary layer is developing. It seems as if the transition occurs at a Reynolds number of about 2 500. However, pressure drop measurements as well as variation in temperature measurements by the same authors (Meyer *et al*., 2009a) and by Olivier (2009), on the same experimental set-up, indicated that transition starts at a Reynolds number of 2 100 and ends at approximately 3 000. The kink in the Nusselt numbers thus indicates the end of transition.

If the results are compared with the Colburn (1933) correlation as modified by Sieder and Tate (1936), all the turbulent regime data (Re>3 000) are predicted on average to within 12%, although they are actually only valid for Reynolds numbers greater than 10 000. For Reynolds numbers greater than 5 000, the correlation predicted the data on average to within 1% with root mean square deviations of 5%, thus validating the experimental set-up for turbulent flow.

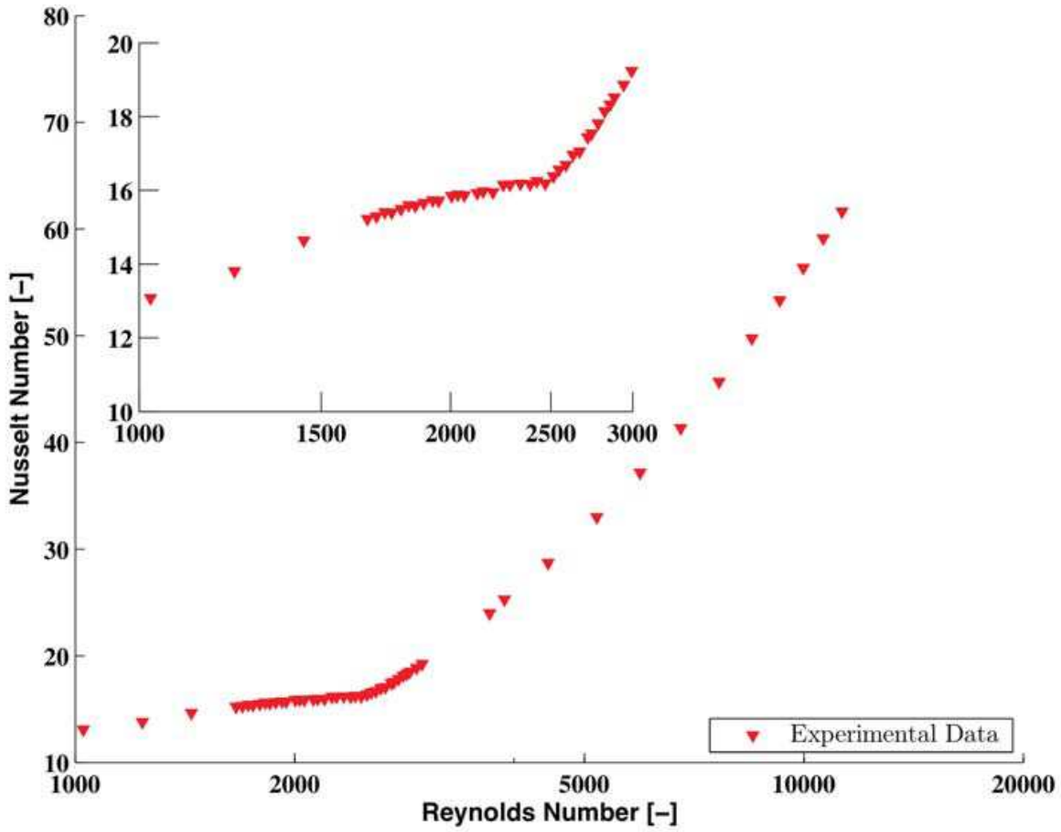

Fig. 7. Heat transfer results for the fully developed smooth tube

Laminar flow results are much higher than predicted by the theoretical constant of 3.66 (ASHRAE, 2009) for the constant wall temperature boundary condition. This is attributed to the buoyancy-induced secondary flow in the tube due to the difference in density at the centre and the wall of the tube. The correlations of Oliver (1962) and those of Shome and Jensen (1995), designed to incorporate these natural convection effects, predicted the laminar data from a Reynolds number of 1 000 to 2 100 to within 10% and 7.5%, respectively. Fig. 8 (Meyer et al., 2009b; Meyer and Olivier, 2010) shows the heat transfer results for the smooth tube with various inlets. Included in the figure is a zoomed-in region covering a Reynolds number range of 1 000 to 3 000. It is apparent that the inlet geometry has no influence on the transition point. In fact, transition for all inlets occurs at the same Reynolds number, that is, it starts at 2 100 and ends at 3 000. The reason for this is that the secondary flows in the tube suppress the growth of the hydrodynamic boundary layer to such a degree that the fluid is fully developed, and hence transition occurs at the fully developed inlet's transition point. This might, however, only be unique to water or low Prandtl number fluids as other researchers have found transition to be dependent on the inlet profile when using a water-glycol mixture together with heat transfer (Ghajar & Tam, 1994). Furthermore, from the data, it is evident that transition from laminar to turbulent flow is not sudden, and there is a smooth transition between the two regimes.

In this instance, the inlet profile also has no influence on the laminar regime, again showing that the natural convection in the tube dominates the flow. Turbulent results also show that there is very little variation in the Nusselt numbers for the various inlet profiles, indicating that in this region the results are independent of the inlet.

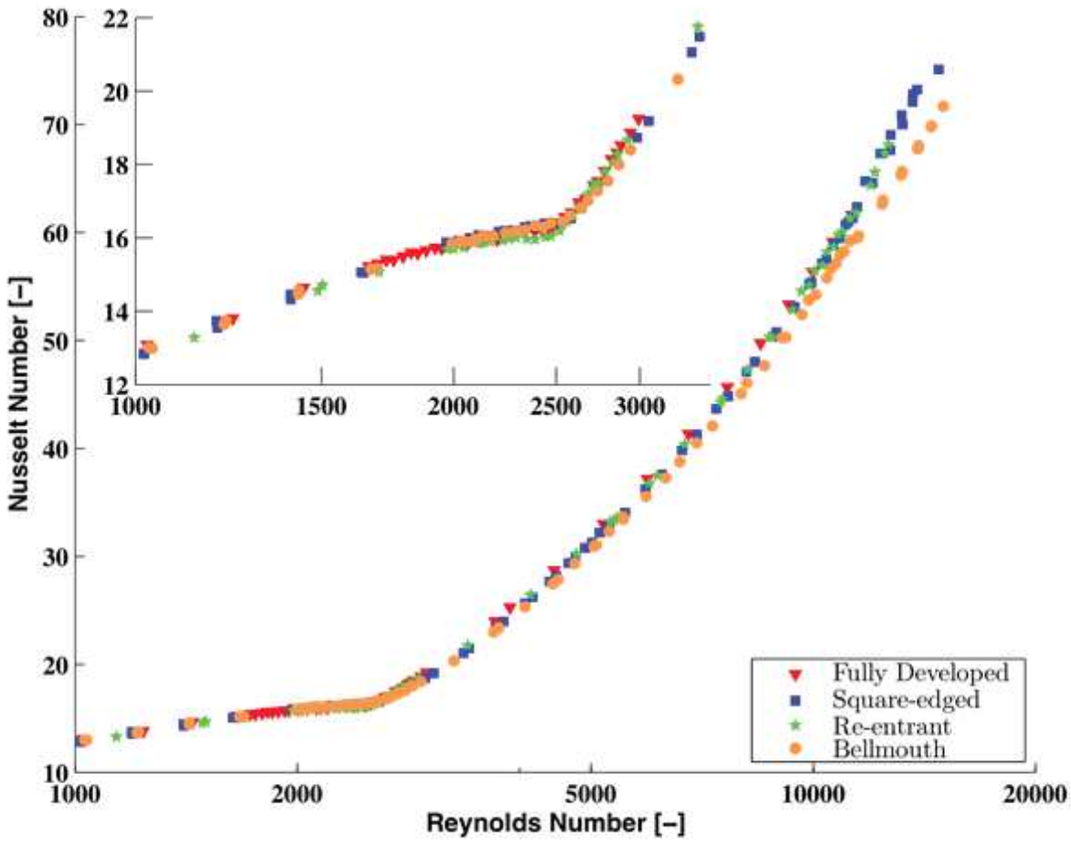

Fig. 8. Heat transfer results for the smooth tube for various inlets

4.4 Friction factor and Nusselt numbers for enhanced tubes

The adiabatic friction factors for enhanced tubes are given in Fig. 9. Also included are the data for the smooth tube for fully developed flow. In general, there is an upward shift in friction factors in the laminar as well as in the turbulent regimes compared with the smooth tube results. Also, transition occurs earlier than for the smooth tube. While the transition for the smooth tube occurs at a Reynolds number of approximately 2 300, it is at 2 000 for the 18° tube and at 1 900 for the 27° enhanced tube. The increase in friction factors is understandable. This is due to the increase in roughness the fins exhibit, which, in turn, increases the resistance to flow. The effects of the different types of inlets are given in Meyer and Olivier (2011a). However, the results in Fig. 9 show that transition occurs earlier with enhanced tubes than with a smooth tube. The more "enhancement", the earlier transition will occur. This also confirms the work of García et al. (2007), who obtained similiar results with wire coil inserts.

Figure 10 shows the fully developed and developing Nusselt numbers for the smooth tube and for the two enhanced tubes with different types of inlets. Turbulent results show that there is a definite increase in heat transfer with the use of the enhanced tubes, with the 27° tube showing the highest enhancement (Meyer and Olivier, 2011b). The 18° tube has more heat transfer enhancement than the smooth tube but a lower heat transfer enhancement than the 27° tube. This is as expected, the more enhancement in the tube with the spiral angle, the more the heat transfer will be increased. However, the results show that the transition Reynolds numbers for all tubes with all the different types of inlets are between 2 000 and 3 000.

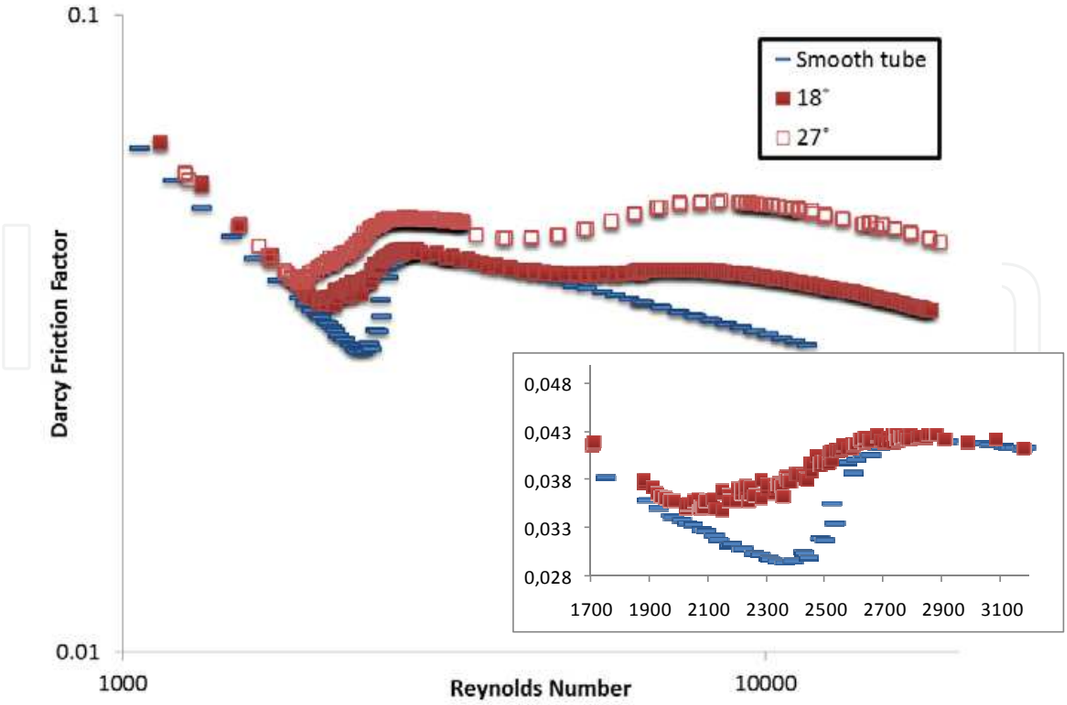

Fig. 9. Fully developed adiabatic friction factors for the enhanced tubes

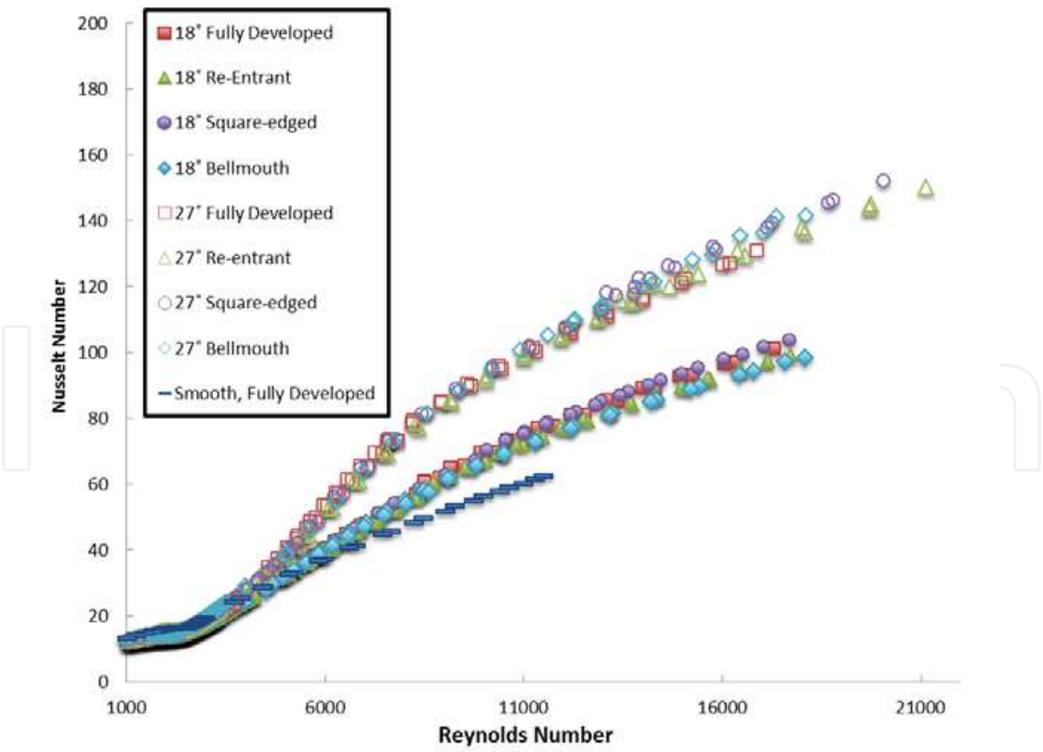

Fig. 10. Heat transfer results for smooth and enhanced tubes for developing and fully developed flow

5. Conclusion

As modern chillers might operate in the transitional flow regime, heat transfer data are needed. Single-phase smooth tube pressure drop and heat transfer measurements for water were conducted in a horizontal circular smooth tube. An experimental set-up consisting of a tube-in-tube counterflow heat exchanger with the cooling of water as the working fluid, was used to obtain measurements within the transitional flow regime. Four different types of inlet geometries were used, i.e. hydrodynamically fully developed, square-edged, re-entrant and bellmouth.

It was found from adiabatic friction factor results that transition from laminar to turbulent flow was strongly dependent on the type of inlet used. The smoother the inlet, the more transition was delayed. Results for the bellmouth inlet showed the largest delay, with transition only occurring at a Reynolds number of approximately 7 000.

On the contrary, diabatic friction factor results showed that transition was independent of the type of inlet. Laminar friction factors were, however, much higher than the values predicted by the Poiseuille relation. This was also attributed to the natural convection flows influencing the boundary layer to such a degree that the shear stress at the tube wall was higher than normal.

Laminar heat transfer results were much higher than their theoretically predicted values due to the secondary flows increasing the amount of mixing in the tube. Furthermore, heat transfer measurements showed that transition with water was totally independent of the type of inlet used and that transition for all the different types of inlets occurred at the same Reynolds number. This was due to the buoyancy-induced secondary flows suppressing the inlet disturbance.

For enhanced tubes without heat transfer, it was found that transition occurs earlier than for smooth tubes and transition occurs earlier than for enhanced tubes. Also, the friction factors of enhanced tubes are higher than those of smooth tubes, as can be expected. With heat transfer it was found that, unlike results obtained from adiabatic flow, inlet disturbances had no effect on the transition. Transition occurs at a Reynolds number of approximately 2 000 to 3 000.

6. Nomenclature

A	Area	m^2
A_i	Inner tube inside heat transfer area	m^2
A_o	Inner tube outside heat transfer area	m^2
Cp	Specific heat	J/kg.°C
D_i	Inner diameter of tube	m
f	Darcy-Weisbach friction factor	
L	Tube length	m
$\dot{m}_i$	Inner-tube fluid mass flow rate	kg/s
$\dot{m}_o$	Annulus fluid mass flow rate	kg/s
Nu	Nusselt number based on D_i	
Pr	Prandtl number	
Δp	Differential pressure drop	Pa

$\dot{Q}_i$	Heat transfer rate for inner-tube fluid	W
Re	Reynolds number based on D_i	
R_w	Tube-wall resistance	˚C /W
T_i	Average fluid temperature for inner tube	˚C
T_o	Average fluid temperature for annulus	˚C
T_{lmtd}	Log-mean temperature difference	˚C
T_{wi}	Temperature of fluid at inner-tube inner wall	˚C
T_{wo}	Temperture of fluid at inner-tube outer wall	˚C
U	Overall heat transfer coefficient	W/m²˚C
u	Average fluid velocity in the inner tube	m/s

Greek symbols

α_i	Heat transfer coefficient of inner tube	W/m²˚C
α_o	Heat transfer coefficient of annulus	W/m²˚C
ρ	Fluid density	kg/m³

Subscripts

in	Inner tube, inlet
out	Inner tube, outlet
hx	Heat transfer
Δp	Pressure drop
out	Outer tube, out

7. References

ASHRAE. (2009). Fluid flow, ASHRAE Handbook - Fundamentals, American Society of Heating, Refrigerating and Air-Conditioning Engineers, Inc., Atlanta

Cengel, Y.A. (2006). *Heat and mass transfer, a practical approach*, (Third edition), McGraw-Hill, Singapore

Colburn, A.P. (1933). A method of correlating forced convection heat transfer data and a comparison with fluid friction, *Transactions of the American Institute of Chemical Engineers*, Vol. 19, pp. 174 - 210

Durst F.; Ray, S., Unsal, B. & Bayoumi, O.A. (2005). The development lengths of laminar pipe and channel flows, *Journal of Fluids Engineering*, Vol., 127, pp. 154-1160

Faris, G.N. & Viskanta, R. (1969). An analysis of laminar combined forced and free convection heat transfer in a horizontal tube, *International Journal of Heat and Mass Transfer*, Vol. 12, pp. 1295-1309

Filonenko, G.K. (1948). On friction factor for a smooth tube, *All Union Thermotechnical Institute*, Izvestija VTI, No. 10, Russia

García, A., Vicente, P.G. & Viedma, A. (2005). Experimental study of heat transfer enhancement with wire coil inserts in laminar-transition-turbulent regimes at different Prandtl numbers, *International Journal of Heat and Mass Transfer*, Vol. 48, pp. 4640 - 4651

García, A., Solano, J.P. Vicente, P.G. & Viedma, A. (2007). Enhancement of laminar and transitional flow heat transfer in tubes by means of wire coil inserts, *International Journal of Heat and Mass Transfer*, Vol. 50, pp. 3176 - 3189

Ghajar, A.J. & Tam, L.M. (1990). Laminar-transition-turbulent forced and mixed convective heat transfer correlations for pipe flows with different inlet configurations, *HTD, Fundamentals of Forced Convective Heat Transfer*, ASME, Vol. 181, pp. 15-23

Ghajar, A.J. & Tam, L.M. (1994). Heat transfer measurements and correlations in the transition region for a circular tube with three different inlet configurations, *Experimental Thermal and Fluid Science*, Vol. 8, pp. 79-90

Ghajar, A.J. & Tam, L.M. (1995). Flow regime maps for a horizontal pipe with uniform wall heat flux and three inlet configurations, *Experimental Thermal and Fluid Science*, Vol. 10, pp. 287- 297

Gnielinski, V. (1976). New Equation for Heat and Mass Transfer in Turbulent Pipe and Channel Flow, *International Chemical Engineering*, Vol. 16, pp. 359–368

Hishida, M., Nagano, Y. & Montesclaros, M.S. (1982). Combined forced and free convection in the entrance region of an isothermally heated horizontal pipe, *Journal of Heat Transfer*, Vol. 104, pp. 153-159

IAPWS. (2003). Uncertainties in Enthalpy for the IAPWS Formulation 1995 for the Thermodynamic Properties of Ordinary Water Substance for General and Scientific Use (IAPWS-95) and the IAPWS Industrial Formulation 1997 for the Thermodynamic Properties of Water and Steam (IAPWS-IF97), Advisory Note No 1

Kline, S.J. & McClintock, F.A. (1953). Describing uncertainties in single-sample experiments, *Mechanical Engineering,* Vol. 75, pp. 3 - 8

Lienhard, J.H. & Lienhard, J.H. (2003). *A Heat Transfer Text Book*, (Third edition), Cambridge: Phlogiston Press

Meyer, J.P., Liebenberg, L. & Olivier, J.A. (2009a). Pressure drop inside a smooth tube with different inlet geometries in the transitional flow regime for water cooled at a constant wall temperature, *Proceedings of the 7th World Conference on Experimental Heat Transfer, Fluid Mechanics and Thermodynamics (ExHFT7)*, Krakow, Poland, pp. 1265 -1272, 28 June to 3 July

Meyer, J.P., Liebenberg, L. & Olivier, J.A. (2009b). Heat transfer characteristics of smooth circular tubes with different inlet geometries in the transitional flow regime, *Proceedings of the 14th IAHR Cooling Tower and Air-Cooled Heat Exchanger Conference*, Stellenbosch, paper number OP05, 1 – 3 December

Meyer, J.P. & Olivier, J.A. (2010). Heat transfer and pressure drop characteristics of circular smooth tubes in the transitional flow regime, *Proceedings of the 19th International Congress of Chemical and Process Engineering CHISA 2010 and the 7th European Congress of Chemical Engineering ECCE7*, Prague, Paper: I6.1, 28 August – 1 September

Meyer, J.P. & Olivier, J.A. (2011a). Transitional flow inside enhanced tubes for fully developed and developing flow with different types of inlet disturbances: Part I – adiabatic pressure drop, *International Journal for Heat and Mass Transfer*, Vol. 54, Issue 7-8, pp. 1587 – 1598

Meyer, J.P. & Olivier, J.A. (2011b). Transitional flow inside enhanced tubes for fully developed and developing flow with different types of inlet disturbances: Part II –

heat transfer, *International Journal for Heat and Mass Transfer*, Vol. 54, Issue 7-8, pp. 1598 – 1607

Mikesell, R.D. (1963). *The Effects of Heat Transfer on the Flow in a Horizontal Pipe,* PhD thesis, Chemical Engineering Department, University of Illinois

Mohammed, H.A. (2009). The effect of different inlet geometries on laminar flow combined convection heat transfer inside a horizontal circular pipe, *Applied Thermal Engineering*, Vol. 29, pp. 581 - 590

Morel, T. (1975). Comprehensive design of axisymmetric wind tunnel contractions, *Journal of Fluids Engineering,* Vol. 97, pp. 225-233

Nunner, W. (1956). Heat transfer and pressure drop in rough tubes, *VDI-Forschungsheft*, 455-B5-39

Obot, N.T., Esen, E.B. & Rabas, T.J. (1990). The role of transition in determining friction and heat transfer in smooth and rough passages, *International Journal of Heat and Mass Transfer*, Vol. 33, No. 10, pp. 2133 - 2143

Obot, N.T., Das, L., Vakili, D.E. & Green, R.A. (1997). Effect of Prandtl number on smooth-tube heat transfer and pressure drop, *International Communications in Heat and Mass Transfer*, Vol. 24, No. 6, pp. 889 – 896

Oliver, D.R. (1962). The effect of natural convection on viscous-flow heat transfer in horizontal tubes, *Chemical Engineering Science*, Vol. 17, pp. 335-350

Olivier, J.A. (2009). *Single-phase heat transfer and pressure drop of water inside horizontal circular smooth and enhanced tubes with different inlet configurations in the transitional flow regime*, PhD thesis, University of Pretoria, Pretoria

Olivier, J.A. & Meyer, J.P. (2010). Single-phase heat transfer and pressure drop of the cooling of water inside smooth tubes for transitional flow with different inlet geometries (RP-1280), *HVAC&R Research*, Vol. 16, No. 4, pp. 471-496

Reynolds, O. (1883). An experimental investigation of the circumstances which determine whether the motion of water shall be direct or sinuous, and the law of resistance in parallel channels, *Philosophical Transactions of the Royal Society of London*, Vol. 174, pp. 935 – 982

Shome, B. & Jensen, M.K. (1995). Mixed convection laminar flow and heat transfer of liquids in isothermal horizontal circular ducts, *International Journal of Heat and Mass Transfer*, Vol. 38, No. 11, pp. 1945-1956

Sieder, E.N. & Tate, G.E. (1936). Heat transfer and pressure drop in liquids in tubes, *Industrial and Engineering Chemistry*, Vol. 28, No. 12, pp. 1429-1435

Tam, L.M. & Ghajar, A.J. (1997). Effect of inlet geometry and heating on the fully developed friction factor in the transition region of a horizontal tube, *Experimental Thermal and Fluid Science*, Vol. 15, pp. 52-64

Wagner, W. & Pruß, A. (2002). The IAPWS formulation 1995 for the thermodynamic properties of ordinary water substance for general and scientific use, *Journal of Physical and Chemical Reference Data*, Vol. 31, pp. 387-535

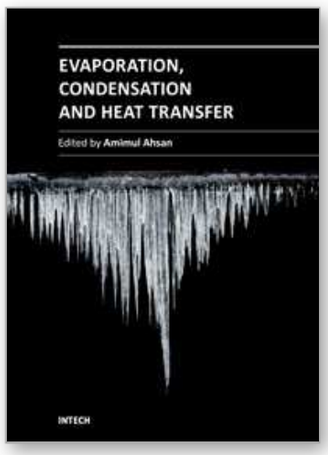

Evaporation, Condensation and Heat transfer
Edited by Dr. Amimul Ahsan

ISBN 978-953-307-583-9
Hard cover, 582 pages
Publisher InTech
Published online 12, September, 2011
Published in print edition September, 2011

The theoretical analysis and modeling of heat and mass transfer rates produced in evaporation and condensation processes are significant issues in a design of wide range of industrial processes and devices. This book includes 25 advanced and revised contributions, and it covers mainly (1) evaporation and boiling, (2) condensation and cooling, (3) heat transfer and exchanger, and (4) fluid and flow. The readers of this book will appreciate the current issues of modeling on evaporation, water vapor condensation, heat transfer and exchanger, and on fluid flow in different aspects. The approaches would be applicable in various industrial purposes as well. The advanced idea and information described here will be fruitful for the readers to find a sustainable solution in an industrialized society.

InTech Europe
University Campus STeP Ri
Slavka Krautzeka 83/A
51000 Rijeka, Croatia
Phone: +385 (51) 770 447
Fax: +385 (51) 686 166
www.intechopen.com

InTech China
Unit 405, Office Block, Hotel Equatorial Shanghai
No.65, Yan An Road (West), Shanghai, 200040, China
中国上海市延安西路65号上海国际贵都大饭店办公楼405单元
Phone: +86-21-62489820
Fax: +86-21-62489821

IntechOpen